**Earthquakes and Structures**, *Vol. 10, No. 3 (2016) 717-733*
DOI: http://dx.doi.org/10.12989/eas.2016.10.3.717


# Seismic evaluation of cemented material dams -A case study of Tobetsu Dam in Japan

Amir Arefian[*1], Ali Noorzad[2a], Mohsen Ghaemian[3b] and Abbas Hosseini[4c]

*[1]Department of Civil Engineering, Science and Research branch, Islamic Azad University, Tehran, Iran*
*[2]Department of Water and Environmental Engineering, Shahid Beheshti University, Tehran, Iran*
*[3]Civil Engineering Department, Sharif University of Technology, Tehran, Iran*
*[4]Department of Civil Engineering, Science and Research branch, Islamic Azad University, Tehran, Iran*

*(Received May 19, 2015, Revised December 13, 2015, Accepted December 14, 2015)*

**Abstract.** Trapezoidal Cemented Sand and Gravel Dam, namely Trapezoid CSG, is a new type of dam. Due to lack of dynamic studies in the field of CSG dam, this research was performed to analyze Trapezoidal CSG dam using dynamic Finite element method with ABAQUS Software. To investigate possible earthquake-induced damages, fragility curves are plotted based on damage index, the length of the cracks created at the dam base and the area of cracked elements in the dam. The seismic analysis indicated that minimum and maximum tensions are generated in the heel and toe of the dam, respectively. According to the fragility curves, with increase in PGA, the possibility of the exceeding the defined limit state is increased. However, the rate of increment is significantly reduced after PGA=0.4 g. Also, the same result is achieved for the second limit state. The "area of cracked elements" is more conservative criterion than the "crack length at the dam base", especially at PGA<0.4 g. As conclusion, CSG dams, despite of being made of poor materials in comparison with concrete dams, show good resistance, and even in some situations, better performance than the weighted concrete dams.

**Keywords:** CSG dam; numerical analysis; fragility curves; concrete damage plasticity; damage index; limit state

## 1. Introduction

The main aim of the current study is to analyze nonlinearly the trapezoid CSG and to investigate seismic response under the influence of earthquake loads. In other words, this research investigates the applicability of fragility curves on the Tobetsu CSG dam as a case study. Further, the safety of the Tobetsu dam was assessed by preparing fragility curves for damage indices. To draw these curves, a number of failures (damage index) and limit state must be produced in order to examine the performance of the dam. Taking advantages of concrete faced rock fill dam

*Corresponding author, Ph.D. Student, E-mail: Amirarefian80@gmail.com
[a]Ph.D., E-mail: a_noorzad@sbu.ac.ir
[b]Ph.D., E-mail: ghaemian@sharif.edu
[c]Ph.D., E-mail: abbas_hoseyni@srbiau.ac.ir


http://www.techno-press.com/journals/eas&subpage=7 ISSN: 2092-7614 (Print), 2092-7622 (Online)

(CFRD) and concrete gravity dam (CGD), cemented sand and gravel (CSG) dams have been the centre of attention as a new type of dam since the late 20th century (Cai *et al.* 2011). The trapezoidal shape of these dams minimizes the tensile stress in the dam body in the severe earthquake loading conditions. Comparing to conventional gravity dams, greater weight of trapezoid-shaped dams provides the safety against landslide, without the requirement for the high shear strength of bedrock (Hirose *et al*. 2001).

As a super lean mix material, the CSG is made of cement, water, and riverbed gravel, or excavation muck devoid of large stones. The use of CSG leads to lower costs of gathering and production of materials. The material production system in trapezoid-shaped dams is much more simplified rather than the aggregate production plant generally required at construction site of concrete dams (Kondo *et al*. 2004). Few studies have been carried out on the applicability of this dam type (Cai *et al.* 2012). In the 1970 s, Yang and Yishan proposed the rudiments of CSG dam constituted by the relatively impervious wall and the fat structure built by low cementing stone in order to keep the dam stable (Yang and Yishan 1981). Londe and Lino in 1992 further described the specifications of the CSG dam type. Compared to RCC dam, Londe found it to be less costly with a higher degree of safety (Londe and Lino 1992). Fujisawa in (2004) discussed the relationship between the strength, stability of trapezoid-Shaped CSG dam and character of CSG material (Fujisawa 2004). Kondo *et al*. (2004) tested the safety of trapezoid-shaped CSG dams during earthquake. Based on the stress distribution inside the dam body, they discussed the influence of the variables dam size and deformability of the ground on the dynamic response during earthquake (Kondo *et al*. 2004). Fujisaki *et al*. (2014) developed a new system to monitor fluctuation trend of the grain size distribution by analyzing the characteristics of fill materials using digital image analysis. They verified the developed system by Tobetsu Dam for rationalization of the quality control during construction (Fujisaki *et al*. 2014). Dam owners are always concerned to maintain favourable conditions even after a disaster like earthquake (Kondo *et al*. 2014). As a useful decision support tool, dam safety risk analysis, could be extremely worthwhile in large applications in dam safety engineering (Altarejos *et al*. 2012). The damage measure depends on the ground motion, the response and the capacity of the building, and the damage index (Colangelo 2008). According to the federal guidelines, risk analysis techniques should be applicable in determining priorities for examination and rehabilitation of dams in terms of safety (FEMA 1979). A set of evaluation scales have been developed to analyze the condition of earth and concrete dams at different modes of internal failure (McCann *et al*. 1983).

Several studies have been carried out on the seismic evaluation of building. Shahriar *et al*. (2012) carried out seismic evaluation of building using multi-criteria decision making method (Shahriar *et al*. 2012). In the 2013 s, Eleftheriadou and Karabinis estimated two different parameters for the description of the seismic demand. After the classification of damaged buildings into structural types they had further categorized according to the level of damage and macro seismic intensity (Eleftheriadou and Karabinis 2013). In the 2015 s, Ebrahimi Nezhad and Poursha described effects of different types of irregularity along the height on the seismic responses of moment resisting frames using nonlinear dynamic analysis (Ebrahimi Nezhad and Poursha, 2015). Roy *et al*. (2015) studies on the effects of accidental eccentricity on the seismic response of four-storey steel buildings laterally stabilized by buckling restrained braced frames conducted (Roy *et al*. 2015). Braga *et al*. (2015) investigated an evaluation of the reliability of the procedure of shake map generation with specific regard to the seismic events that struck the Emilia region on May 20 and 29, 2012 (Braga *et al*. 2015). So far the study, have not been carried out on the seismic evaluation of CSG dam.

The failure probability of an engineered structure against a particular hazard could be depicted by fragility curves (Ellingwood and Tekie 2001). The fragility curves are useful in predicting the extent of probable damages (Karim and Yamazaki 2003). It represents the damage possibility of structures as a result of various ground shakings (Nateghi and Shahsavar 2004).

The Peak Ground Acceleration (PGA) or Peak Ground Velocity (PGV) is usually used to present the earthquake intensity on the ground (Al Abadi *et al*. 2006). Kennedy *et al*. (1980) plotted fragility curves for nuclear power plants. In 1994, Anagnos et al followed the ATC-13 criteria to draw fragility curves in order to test the structures in California (Anagnos and Rojahn 1980). The fragility curves are widely used in retrofitting of dams. Damage index (DI) is a physical value that estimates damages imposed to a structure and correlates with a critical state in a structure (Mita and Takahira 2004). The idea of quantitative describing of the damage state of a structure on a defined scale is attractive due to its simplicity (Ghobarah *et al*. 1999). The DI values could be normalized as zero value when the structure is in no damage state and a unit value when failure or total collapse of the structure happens (Alembagheri and Ghaemian 2012).

Despite of the use of fragility curves for structures such as frames, tanks, nuclear power plants, and bridges have been initiated from many years and even decades ago, however, applicability of these curves for dams is a new concept. The first study on seismic fragility curves was carried out by Tekie and Ellingwood in 2003 for a concrete dam (Bluestone Dam). This dam was analyzed by a linear spectral model and the fragility curves were prepared based on tensile stress in the heel and the neck of the dam, the possibility of landslide, and displacement of dam crest on the basis of ascending PGAs (Tekie and Ellingwood 2003). In 2007, Lin and Adams prepared seismic fragility curves for the dams in eastern- and western Canada (Lin and Adams 2007). Ghaemian and Kashani conducted studies on the plotting of fragility curve in 2008. Using two parameters of the area of cracked elements and the length of cracked elements on the Pine flat dam, they specified earthquake induced failure. In their study it was shown that considering linear behaviour for the foundation and mass less assuming of foundation would be better, upon which the design is more conservative (Kashani and Ghaemian 2009).

## 2. Methodology

### 2.1 Numerical modeling

The case study dam in this research is Tobetsu dam located in Hokkaido region, Japan. This dam is constructed on Toubetsu River as a tributary of Ishikari River. The numerical approach was used for seismic assessment of the Toubetsu dam. So, the tallest non-overflow section of the dam was evaluated using finite element method. Table 1 provides the main features of the Toubetsu dam.

Fig. 1 depicts the tallest monolith of the dam used for the seismic analysis. The finite element mesh of the dam, truncated reservoir, and foundation are illustrated in Fig. 2.

Due to the high similarity to concrete gravity dams, there could be found two major failure modes with the Trapezoid CSG dams, including “tensile overstressing and sliding along cracked surfaces in the dam body or at the dam bottom”, and “foundation interface or planes of weakness within the foundation” (Ghanaat 2004). It is worth mentioning that sliding and overturning failures rarely occur in concrete gravity dams (Fishman 2009). Accordingly, this paper was carried out to address the overstressing failure mode of the Toubetsu dam using Abaqus Software. No sign of sliding plane was found within the dam body or at the dam-foundation interface. So, the geometry of the model was initially created, which includes of two parts; "water" and "dam and foundation". The physical specifications of the dam are given in Table 2.

Table 1 Main features of the Toubetsu dam

| Item | | Specification |
|---|---|---|
| | Location | Hokkaido region (Toubetsu Town. Ishikari-gun, Hokkaido) |
| | River | Toubetsu River, a tributary of the Ishikari River |
| | Catchment area ($km^2$) | 231.1 |
| | Completed | 2012 |
| Reservoir | Total storage capacity ($10^6$ $m^3$) | 74.5 |
| | Effective storage capacity ($10^6$ $m^3$) | 66.5 |
| | Reservoir area ($km^2$) | 5.8 |
| Dam | Structure type | Trapezoidal CSG dam |
| | Height (m) | 52 |
| | Length of crest (m) | 432 |
| | Volume ($10^3$ $m^3$) | 813 |
| Spillways | Emergency spillway | Free overflow, 1.9 m * 13 m, 6 gates |
| | Spillway | Natural control with flow notches , 5.4 m * 15 m, 4 gates Natural control with flow notches, 5.4 * 5 m, 1 gates |
| | Overflow length (m) | 117 |
| | Design flood ($m^3$/s) | 2400 |

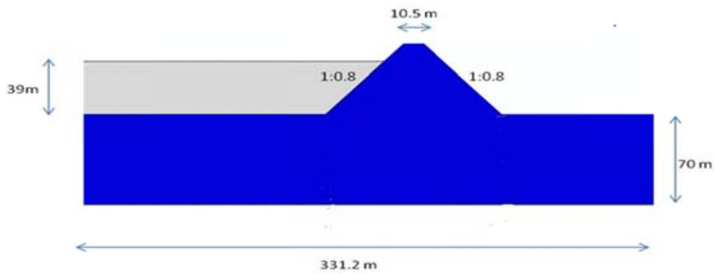


Fig. 1 Dimensions of the tallest monolith of Toubetsu Dam

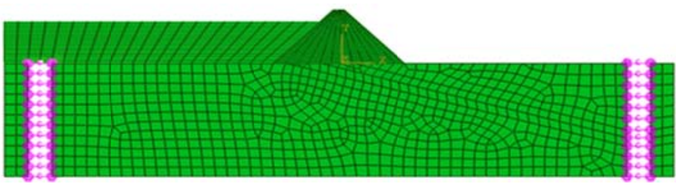

Fig. 2 Finite element model of the tallest monolith of Toubetsu Dam

Table 2 Physical specifications of Toubetsu dam

| Specifications of CSG materials | |
|---|---|
| Mass Density | $24\ ^{kN}/_{m^3}$ |
| Elasticity | |
| Young Modulus | $26.45e5\ ^{kN}/_{m}\ 2$ |
| Poisson's coefficient | 0.167 |
| Plasticity | |
| Dilation Angle | 15° |
| Eccentricity | 0.1 |
| $^{fb_0}/_{fc_0}$ | 1.16 |
| K | 0.666 |
| Viscosity Parameter | 0 |

The acoustic water was assumed with a bulk modulus of 2.2 e9 and a density of 10 $^{kN}/_{m^3}$. To calculate the damping coefficients of α and β, first and second natural frequencies were calculated and placed in Eq. (1)

$$\xi_i = \frac{\alpha}{2w_i} + \frac{\beta w_i}{2} \tag{1}$$

Where $\xi_i$=Rayleigh Damping of the whole system, $\alpha, \beta$=damping coefficients and $w_i$ =natural frequencies of the system. These parameters, for dam foundation, are as follows

$$\rho=19\ ^{kN}/_{m^3} \qquad E=2e^7\ ^{kN}/_{m^2} \qquad \nu=0.3$$

The Lysmer boundary conditions were considered and the hardness of dashpots was calculated using the Eqs. (2)-(5)

$$G=\rho V_s^2 \tag{2}$$

$$V_p = 2V_s \tag{3}$$

$$K_P = \rho V_P A \tag{4}$$

$$K_s = \frac{K_P}{2} \tag{5}$$

Where $V_s$ is the shear wave velocity in soil and $V_P$ is the normal wave velocity in the soil.

### *2.2 Constitutive model*

The CDP (concrete damage plasticity) constitutive model was used to model the behavior of dam body materials. The behavior of foundation materials was modeled by Mohr-Coulomb constitutive model. The CDP model provides the overall capability to model concrete and other pseudo-fragile materials in all types of structures (beams, trusses, skins, and solids). This constitutive model is a damaged and model based on plasticity of concrete. It is assumed that two main failure mechanisms are strain cracking and crushing compression of concrete materials.

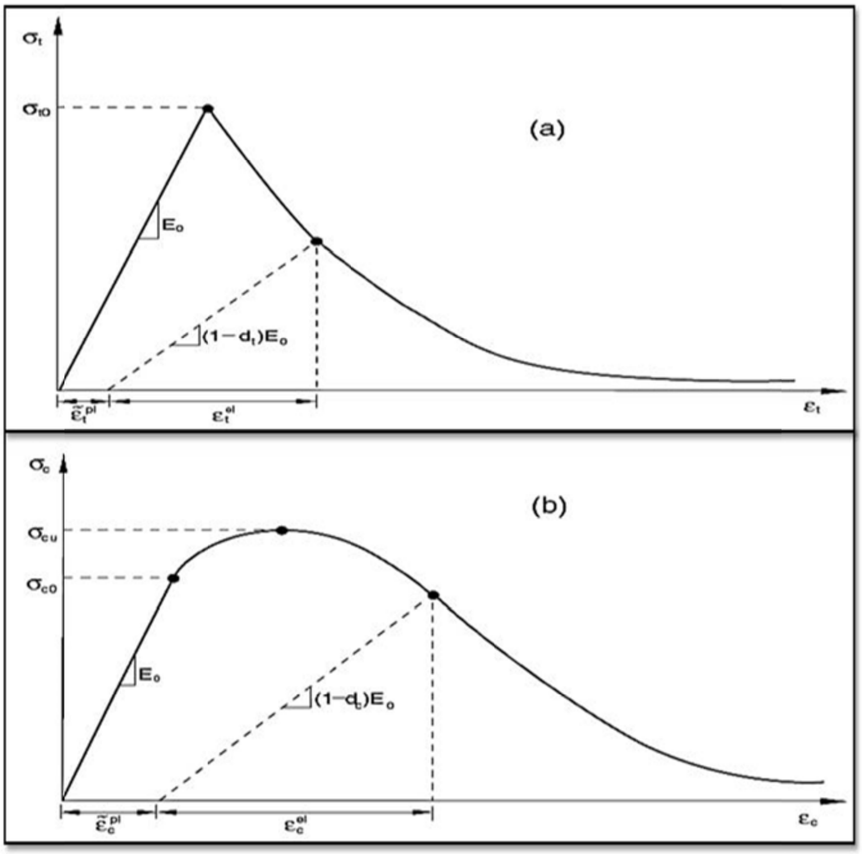


Fig. 3 Concrete response under uniaxial compressive loading (a), uniaxial strain loading (b)

According to Fig. 3, it is assumed that uniaxial stress-strain response of concrete is determined by the damaged plasticity.

### 2.3 Mohr - Coulomb Model

The most important theory in relation to the anticipation of soil failure is Mohr-Coulomb yield criterion. The basis of this theory is the relationship between vertical stress and shear stress on a sheet called failure sheet. Mohr - Coulomb failure line is a straight line tangent to Mohr circles. Fig. 4 illustrates Mohr - Coulomb failure envelope in the linear mode. Accordingly, the Mohr - Coulomb criterion could be written as below (Eq. (6))

$$\tau = c + \sigma \tan \phi \tag{6}$$

Where $\tau$=shear stress, $\sigma$=normal stress (negative under compression), $c$=cohesion of materials, and $\phi$= friction angle of materials.

Mohr - Coulomb model in ABAQUS Software considers a linear relationship between shear stress and compression stress. Mohr - Coulomb model assumes that failure is independent of the

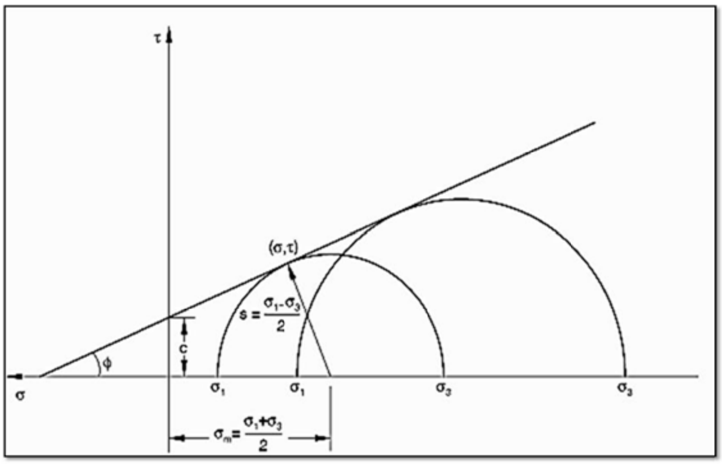


Fig. 4 Mohr - Coulomb failure envelope

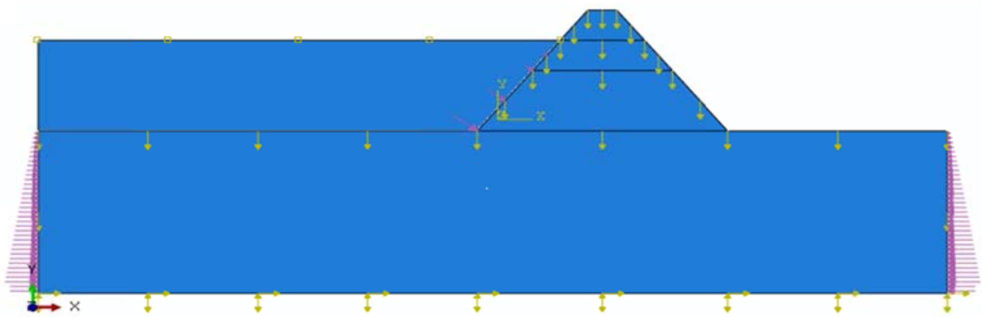

Fig. 5 Lateral forces imposed on the foundation sides

amount of intermediate stress. In this paper, the constitutive Mohr - Coulomb model was used to model the behavior of foundation materials. The Mohr - Coulomb model of the ABAQUS Software is an elastoplastic model with a yield function that includes isotropic hardening and softening in cohesion. However, this model makes use of the potential function in the hyperbolic form, which has no corner on the diatonic sheet. Since the function is completely smooth, it presents a specific definition of the direction of plastic flow.

### *2.4 Static analysis*

After completing the steps to construct the model, a static analysis is initially performed to calculate the lateral forces imposed on the foundation sides (Fig. 5).

### *2.5 Probabilistic safety assessment*

To plot fragility curves, the model should be analyzed at least for three earthquakes. In this research, the model was analyzed for five earthquakes, including Northridge, Loma Perita, Kocaely, Duzci, and Sanfernando. This job was done using Seismosignal Software. For this purpose, the records of the earthquakes were normalized by PGAs. Accordingly, the outputs were based on the PGA values of 0.1 g, 0.2 g, 0.3 g, 0.4 g, 0.5 g, 0.6 g, 0.7 g, and 1 g. For dam safety analysis, some limit states should be defined to test the dam performance. For example, this limit state for frames should be drift of stories, rotation of nodes, and so on. To plot the seismic fragility curves, it should be considered the probability of exceeding to this structural limit state. The fragility in Eq. (7) addresses the probability of Engineering Demand Parameter (EDP) exceeding structural limit state (LS) at the defined PGA

$$\text{Fragility}=P[EDP>LS|PGA] \tag{7}$$

The probability could also be expressed by lognormal distribution in Eq. (8)

$$\text{Fragility}=P[EDP>LS|PGA]=1-P[EDP<LS|PGA]=1-\Phi[\frac{\ln(LS)-\mu}{\sigma}] \tag{8}$$

Where $\Phi$=standard normal probability integral, $\mu$=mean of data and $\sigma$=logarithmic standard deviation

Two factors of the first limit state (LS1) and the second structural limit state (LS2) should be calculated to develop fragility curves for concrete gravity dams. The LS1 is defined as the crack length at the base (usually equals to about 0.26 of the base length of dam.

The LS2 addresses the total areas of cracked elements in the dam body, which approximately 0.0195 of the tallest monolith section (Mirzahosseinkashani and Ghaemian 2009).

At the end, for validation of the model, the crack length at the base was analyzed using ANSYS Software. Afterwards, the results of two models were compared, statistically.

## 3. Results

### 3.1 Nonlinear dynamic analysis results by ABAQUS

For dynamic analysis, the dam was tested by five earthquakes, including Duzci, Kocaeli, Loma Perita, Northridge, and Sanfernando. The records of the earthquakes are depicted in Figs. 6-11.

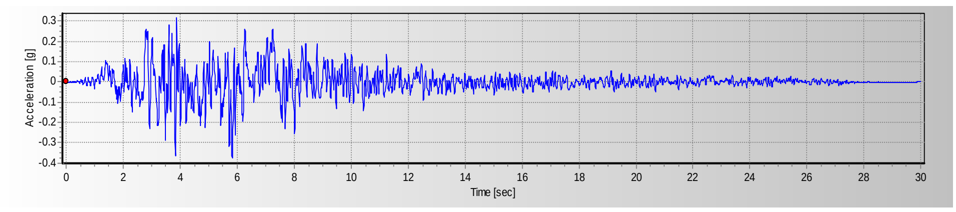


Fig. 6 Accelerograph of the Kocaeli earthquake

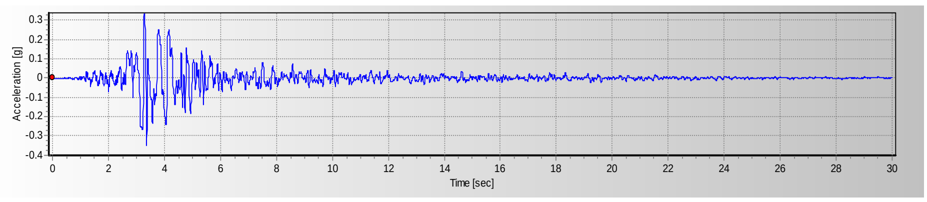


Fig. 7 Accelerograph of Loma Perita earthquake

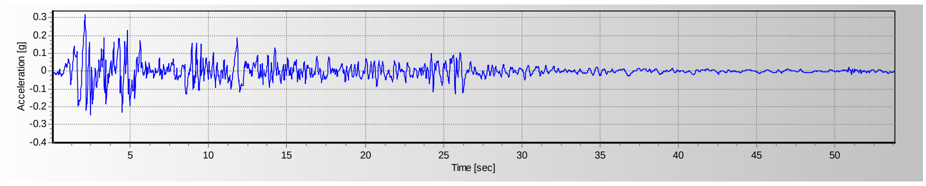


Fig. 8 Accelerograph of Elcentro earthquake

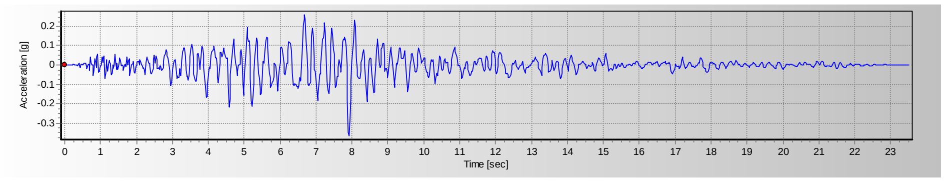


Fig. 9 Accelerograph of Northridge earthquake

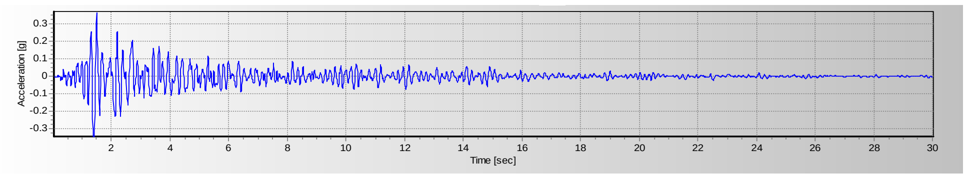


Fig. 10 Accelerograph of San Fernando earthquake

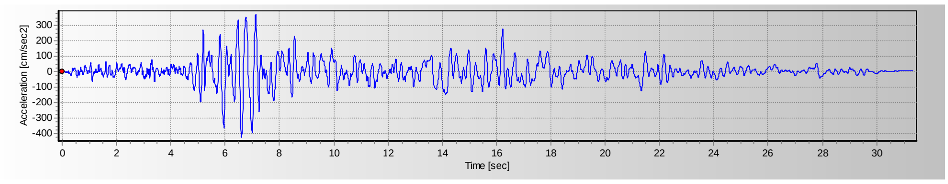


Fig. 11 Accelerograph of Duzce earthquake

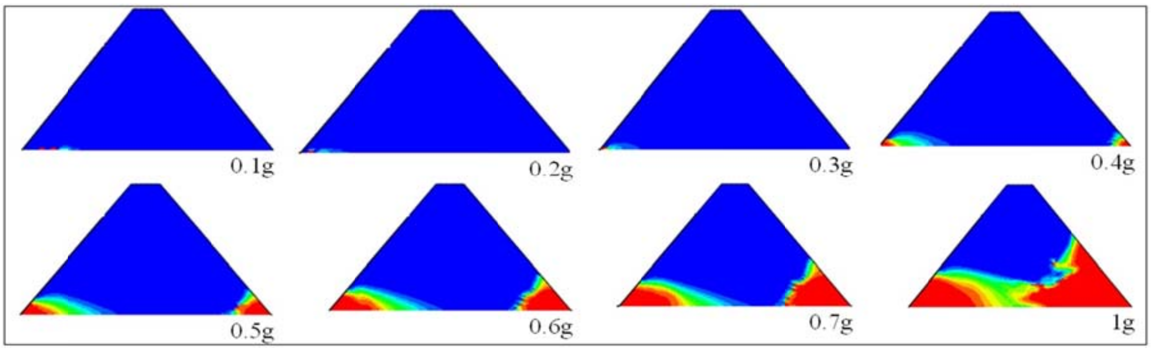


Fig. 12 The propagation of cracks in the dam body subjected to Duzci earthquake

The outputs of nonlinear dynamic analysis subjected to the five earthquakes are demonstrated in Figs. 12-16.

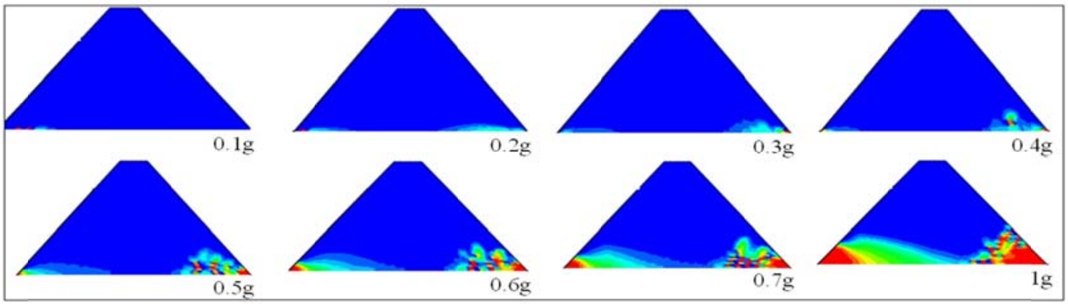


Fig. 13 The propagation of cracks in the dam body subjected to Kocaeli earthquake

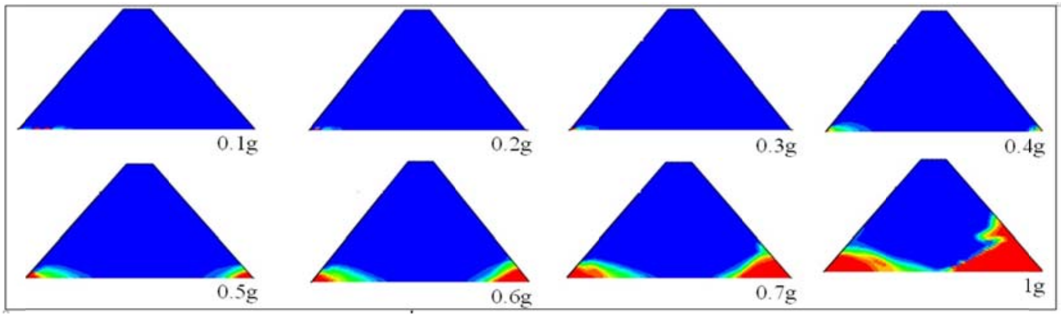


Fig. 14 The propagation of cracks in the dam body subjected to Loma Perita earthquake

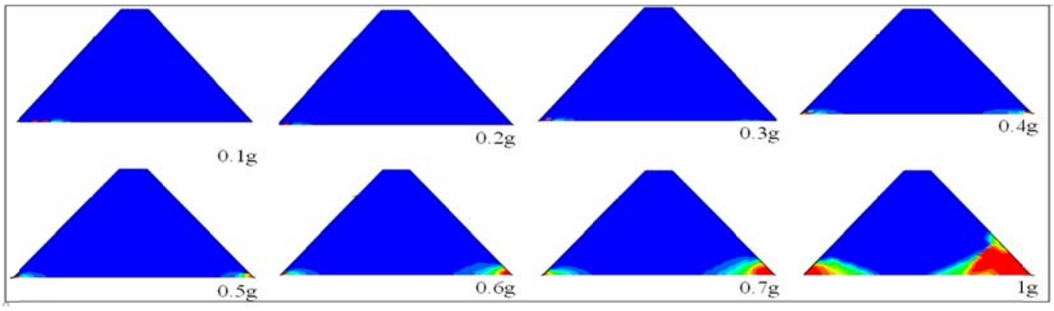


Fig. 15 The propagation of cracks in the dam body subjected to Northridge earthquake

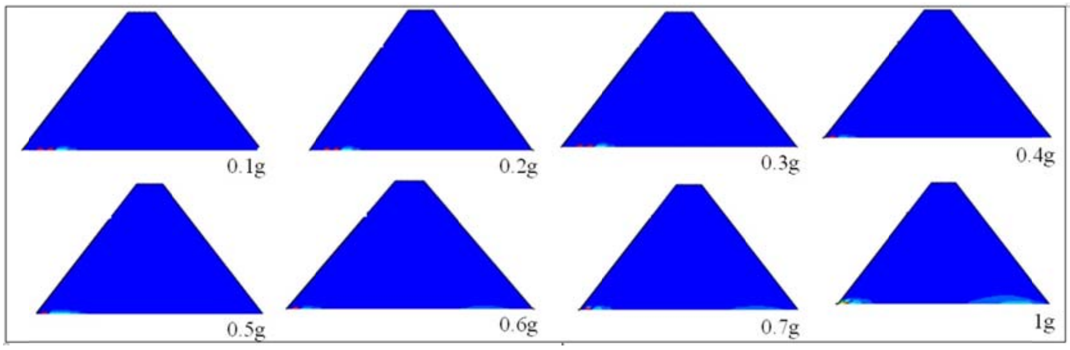


Fig. 16 The propagation of cracks in the dam body subjected to Sanfernando earthquake

The crack length at the dam base for the five earthquakes with 8 different PGAs is presented in Table 3.

For statistical analysis of the results from ABAQUS and ANSYS software and ensure of the obtained results, the Kolmogorov-Smirnov test (K-S test) in SPSS software was used.

Table 3 Crack length at the toe and heel of the dam calculated by ABAQUS Software

| *Earthquake* intensity | PGA | | | | | | | | |
|---|---|---|---|---|---|---|---|---|---|
| | 0.1g | 0.2g | 0.3g | 0.4g | 0.5g | 0.6g | 0.7g | 1g | LS1 |
| DUZ | 11.86 | 13.85 | 13.87 | 33.67 | 53.52 | 67.4 | 81.27 | 91.2 | 23.712 |
| KOC | 11.86 | 29.5 | 49.6 | 41.66 | 67.4 | 75.3 | 91.2 | 91.2 | |
| LOMA | 15.82 | 11.89 | 11.89 | 25.77 | 45.59 | 57.5 | 67.4 | 91.2 | |
| NOR | 11.86 | 11.89 | 11.89 | 35.68 | 25.78 | 37.66 | 47.6 | 71.3 | |
| SAN | 11.89 | 11.9 | 12 | 17.84 | 24 | 27.7 | 33.69 | 49.56 | |
| Arithmetic mean | 12.658 | 15.806 | 19.85 | 30.924 | 43.258 | 53.112 | 64.232 | 78.892 | |
| Var | 3.12462 | 59.3196 | 277.2922 | 85.794 | 342.484 | 400.061 | 559.26 | 343.12 | |
| Standard Deviation | 1.767659 | 7.70192 | 16.65209 | 9.2625 | 18.5063 | 20.0015 | 23.649 | 18.523 | |
| P(X>XI)=LS | 2.01E-10 | 0.15233 | 0.408299 | 0.7819 | 0.85456 | 0.9292 | 0.9567 | 0.9986 | |

In order to verify the simulation results of the ABAQUS, the crack length at the dam base was calculated once again by ANSYS to compare the obtained results. Table 4 provides the data of crack length at the toe and heel of the dam calculated by ANSYS

Table 4 Crack length at the toe and heel of dam calculated by Ansys Software

| Earthquake intensity | PGA | | | | | | | |
|---|---|---|---|---|---|---|---|---|
| | 0.1 g | 0.2 g | 0.3 g | 0.4 g | 0.5 g | 0.6 g | 0.7 g | 1 g |
| DUZ | 10.97 | 13.45 | 13.28 | 33.28 | 52.59 | 66.59 | 80.51 | 90.54 |
| KOC | 10.91 | 29.16 | 48.78 | 41.27 | 66.21 | 74.15 | 90.14 | 90.12 |
| LOMA | 14.89 | 11.34 | 11.3 | 25.38 | 44.66 | 56.78 | 66.64 | 90.32 |
| NOR | 10.97 | 11.55 | 11.21 | 35.29 | 24.58 | 36.85 | 46.34 | 70.32 |
| SAN | 11 | 11.56 | 11.41 | 17.45 | 23.07 | 26.89 | 32.12 | 48.9 |

#### *3.1.1 Kolmogorov-Smirnov test results*

The results of K-S test for the PGA parameter are presented in Table 5. If the type I error is desired to be 0.05 and statistical significance (Sig) is the basis for the judgment, then, due to the Sig value of 0.037, the difference between the mean PGA values will be significant. If the value of type I error is 0.05 and Z test is the basis for the judgment, then, the difference between the mean PGA values of two models will be insignificant, since the z score of 1.432 is less than the critical value ($Z_{0.975}$=1.96) . If the value of type I error is 0.01 and the statistical significance (Sig) is the basis for the judgment, then, the difference between the mean PGA values of two models will be insignificant, because the Sig. value (0.037) exceeds 0.01. If the value of type I error is 0.01 and the Z test is the basis for judging, then, the difference between the mean PGA values of two models will be insignificant whereas the z score of 1.432 is less than the critical value ($Z_{0.995}$=2.57). According to the statistical results, the outputs of the ABAQUS are verified and reliable.

### *3.2 Fragility curve plotting*

#### *3.2.1 Fragility curve plotting based on LS1*

LS1=0.26* Dams base length

Using the content of Table 3, the fragility curve is illustrated for the LS1 (the length of crack at the base) in Fig. 17.

Table 5 Results of two-sample KS test on the PGA outputs modeled by ABAQUS and ANSYS software, Tobetsu dam

| Statistically significant (Sig) | Z score |
|---|---|
| 0/037 | 1/432 |

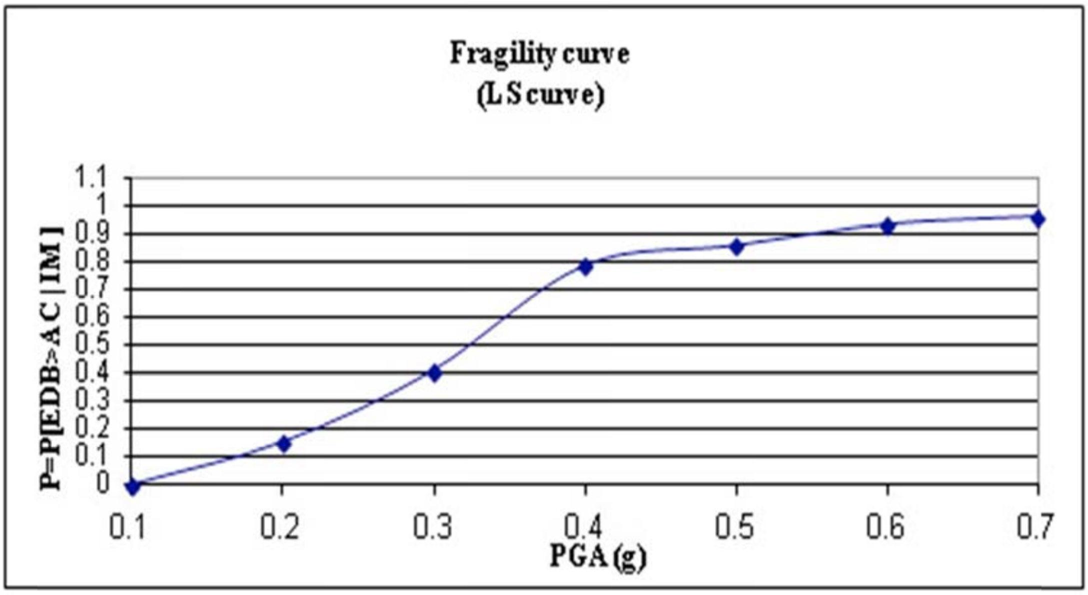


Fig. 17 Seismic fragility curves based on the length of crack at the base

According to the curve, the possibility of exceeding beyond the LS is increased until the PGA=0.4 g, and since after that the increment is slow.

### *3.2.2 Fragility curve plotting based on LS2*

LS2=0.0195* tallest monolith section of dam

The areas of cracked elements in Tobetsu dam for five earthquakes with 8 PGAs are given in Table 6.

The fragility curve for the LS2 (total area of cracked elements in the dam body) is demonstrated in Fig. 18.

Table 6 Areas of cracked elements at the body of dam

| Earthquake intensity | PGA | | | | | | | | LS2 |
|---|---|---|---|---|---|---|---|---|---|
| | 0.1 g | 0.2 g | 0.3 g | 0.4 g | 0.5 g | 0.6 g | 0.7 g | 1 g | |
| DUZ | 15.8 | 18.05 | 31.6 | 154.6 | 343.1 | 580 | 887 | 1320.18 | 51.56 |
| KOC | 15.2 | 119.6 | 162.5 | 178 | 437.9 | 623 | 624 | 813 | |
| LOMA | 17.19 | 16.24 | 20 | 70.7 | 201.5 | 324.8 | 468 | 806.3 | |
| NOR | 13.37 | 15.89 | 16.24 | 68.4 | 100.1 | 141.4 | 246 | 410.8 | |
| SAN | 15.3 | 16.9 | 21 | 17.84 | 18.4 | 23.88 | 39.7 | 113.68 | |
| Mean | 15.372 | 37.336 | 50.268 | 97.91 | 220.2 | 338.62 | 453 | 692.792 | |
| Var. | 1.88277 | 2115.479 | 3968.797 | 4413 | 29498 | 69321 | 402 | 208960 | |
| Standard Deviation | 1.3721407 | 45.99434 | 62.99839 | 66.43 | 171.7 | 263.29 | 329 | 457.121 | |
| P(X>XI)=LS | 0 | 0.378564 | 0.491819 | 0.757 | 0.837 | 0.8622 | 0.89 | 0.91966 | |

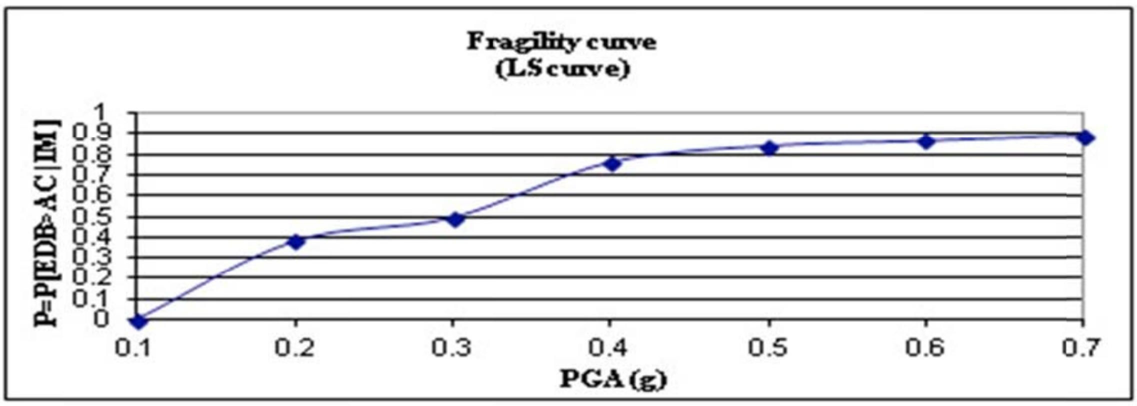


Fig. 18 Seismic fragility curves based on the areas of cracked elements

According to Fig. 18, the possibility of exceeding of cracked areas in the dam body beyond the LS is high at the PGA of 0.4 g, but after 0.4 g the increase rate is significantly reduced.

## 4. Discussions

In this research the behaviour of Tobetsu Dam against 5 different earthquakes with 8 PGA values were studied using nonlinear dynamic analysis. Figs. 17 and 18 are depicted in a diagram in Fig. 19 Based on the results, the increment rate of occurrence probability of LS2 is greater in comparison with LS1 until PGA=0.4 g. However after this point which both LS1 and LS2 have the same probability values, the increment rate of occurrence probability of LS1 is merely more than LS2.

Therefore, the fragility curves based on the LS2 could grant structural safety of the dam even under the near-field earthquakes. In Fig. 20, the fragility curve of Tobetsu dam is compared with Blue Stone dam and Pine Flat dam. The LS, in all of the three curves, refers to the crack length at the dam base. The occurrence probability of LS in Tobetsu Dam is greater than Blue Stone Dam, but less than Pine Flat Dam.

Ignoring the impact of water, the probability of exceeding beyond the LS is lower in Blue Stone Dam. Due to the trapezoidal shape of the Tobetsu dam and consequently, less tension stress than

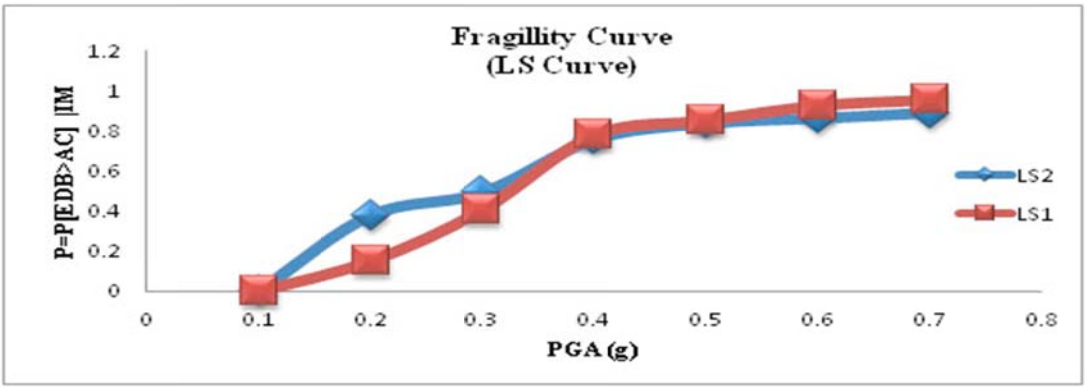


Fig. 19 Comparing the fragility curves plotted based on LS1 and LS2

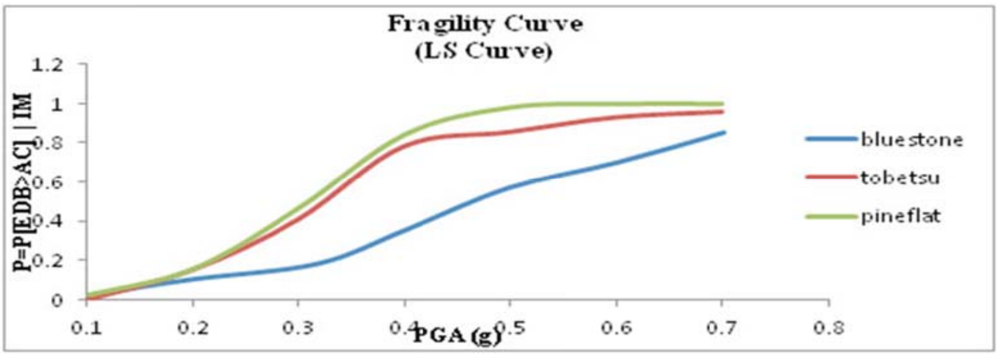


Fig. 20 Seismic fragility curves based on crack length at the base

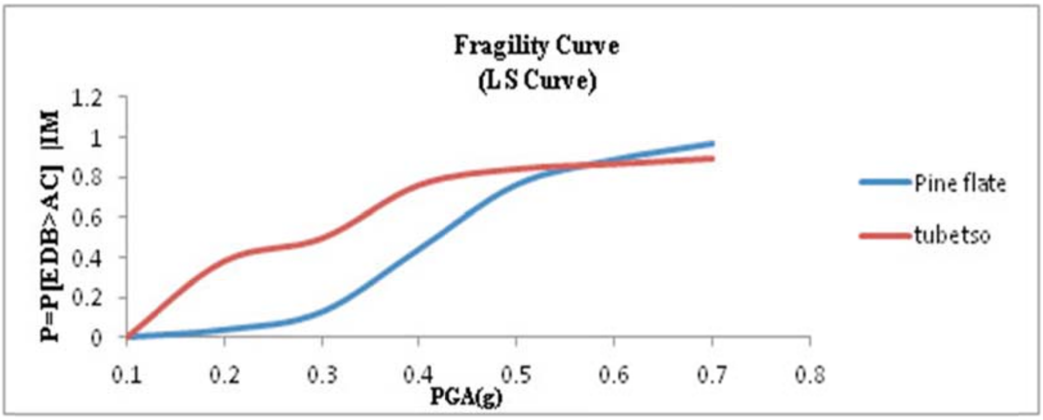


Fig. 21 Seismic fragility curves based on areas of cracked elements

concrete gravity dams, the possibility of exceeding of crack length beyond the LS will be lower than Pine Flat. Fig. 21 compares the fragility curve of Tobetsu dam against Pine Flat dam. The LS represents the area of cracked elements at both curves. According to the Fig. 20, up to the PGA=0.55, the occurrence probability of LS in Tobetsu Dam is greater and since then, the portability rate would decreased. Because of the lower strength of the body materials, the area of the cracked elements at Tobetsu Dam is greater than Pine Flat Dam. Thus, the probability of exceeding from defined LS would be higher.

## 5. Conclusions

This paper describes the characteristics of a trapezoid-shaped dam based on the results of the nonlinear stress analysis by finite element method and fragility curves. The following conclusion may be drawn:

The detailed analysis seems necessary before and while designing and constructing specific trapezoid-shaped CSG dams to check the properties of dam materials.

Maximum tension stress is imposed to the toe and heel of the dam.

The failure initially occurs at dam heel and then extent to the toe. However, the failure of the toe region is wider than the heel. Two LS values of LS1=0.26 (crack length at dam base) and LS2=0.0195 (area of cracked elements in dam body) suit to plot fragility curves of trapezoid-shaped CDM dams. The LS2 is more conservative criterion than the LS1, particularly at PGA<0.4.

Comparing the fragility curves of the Tobetsu CSG Dam with that of concrete gravity dams reveals the fact that CSG dams, in spite of being made of lower strength materials, show good resistance, in some occasions, better than concrete gravity dams. This could be partly due to the shape of these dams and the trapezoidal shape of their cross section.

## References

Al Abadi, H., Lam, N.T.K. and Gad, E. (2006), "Seismic fragility curves for damage to building contents", *J.*

*Earthq. Eng*., 161-168.

Alembagheri, M. and Ghaemian, M. (2012), "Seismic assessment of concrete gravity dams using capacity estimation and damage indexes", *Earthq. Eng. Struct. Dyn*., **42**(1), 123-144.

Altarejos, L., Escuder, I., Serrano, A. and Morales, A. (2012), *Factor of safety and probability of failure in concrete dams*, Risk Analysis, Dam Safety, Dam Security and Critical Infrastructure Management, Taylor & Francis Group, London.

Anagnos, T., Rojahn, C. and Kiremidjian, A.S. (1994), "Building fragility relationships for California", *Fifth U.S. National Conference on Earthquake Engineering*, 4, Chicago, USA.

Braga, F., Gigliotti, R., Monti, G., Morelli, F., Nuti, C., Salvatore, W. and Vanzi, I. (2015), "Post-Seismic assessment of existing constructions: Evaluation of the shakemaps for identifying exclusion zones in Emilia", *Eartq. Struct.*, **8**(1), 37-56.

Cai, X., Wu, Y., Guo, X. and Ming, Y. (2012), "Research review of the cement sand and gravel (CSG) dam", *Front. Struct. Civ. Eng*., **6**(1), 19-24.

Cai, X., Wu, Y., Yi, J. and Ming, Y. (2011), "Research on shape optimization of CSG dams", *Water Sci. Eng.*, **4**(4), 445-454.

Colangelo, F. (2008), "On the computation of seismic fragility curves", *Conference on Earthquake Engineering*, Beijing, China.

Ebrahimi Nezhad, M. and Poursha, M. (2015), "Seismic evaluation of vertically irregular building frames with stiffness, strength, combined-stiffness-and-strength and mass irregularities", *Earthq. Struct*., **9**(2), 353-373.

Eleftheriadou, A. and Karabinis, A. (2013), "Evaluation of damage probability matrices from observational seismic damage data", *Earthq. Struct*., **4**(3), 229-324.

Ellingwood, B. and Tekie, B. (2001), "Fragility analysis of concrete gravity dam", *J. Infrastruct. Syst.*, **7**(2), 41-48.

Federal Emergency Management Agency, Interagency Committee on Dam Safety (1979), *Federal Guidelines for Dam Safety*, Federal Coordinating Council for Science, Engineering, and Technology, Washington, DC.

Fishman, Y. (2009), "Stability of concrete retaining structures and their interface with rock foundations", *Rock Mech. Min. Sci.*, **46**(6), 957-966.

Fujisaki, K., Kawano, K. and Kuronuma, I. and Takei, A. (2014), "Fluctuation monitoring system for grain size distribution of cemented sand and gravel materials using digital image analysis", *International Symposium on Dams in Global Environmental Challenges*, Bali, Indonesia.

Fujisawa, T. (2004), "Material properties of CSG for the seismic design of trapezoid-shaped CSG dam", *13th World Conference on Earthquake Engineering*, Vancouver, Canada.

Ghanaat, Y. (2004), "Failure modes approach to safety evaluation of dams", *Proceedings of 13thWorld Conference on Earthquake Engineering*, Vancouver, Canada.

Ghobarah, A., Abou-Elfath, H. and Biddah, A. (1999), "Response-based damage assessment of structures", *Earthq. Eng. Struct. Dyn.*, **28**(1), 79-104.

Hirose, T., Fujisawa, T. and Nagayama, I., Yoshida, H. and Sasaki, T. (2001), "Design criteria for trapezoid-shaped CSG dams", *ICOLD Workshop*, Germany.

Karim, K.R. and Yamazak, F. (2003), "A simplified method of constructing fragility curves for highway bridges", *Earthq. Eng. Struct. Dyn.*, **32**(10), 1603-1626.

Kennedy, R.P., Cornell, C.A., Campbell, R.D., Kaplan, S. and Perla, H.F. (1980), "Probabilistic seismic safety study of an existing nuclear power plant", *Nuclear Eng. Des.*, **59**(2), 315-338.

Kondo, M., Sasaki, T. and Kawasaki, H. (2004), "Characteristics of stress distribution in trapezoid-shaped CSG dam during earthquake", *13th World Conference on Earthquake Engineering*, Vancouver, Canada.

Kondo, M., Shida, T. and Enomura, T. (2014), "Dynamic analysis of seismic behavior of raised concrete gravity dam", *International Symposium on Dams in Global Environmental Challenges*, Bali, Indonesia.

Lin, L. and Adams, J. (2007), "Lessons for the fragility of Canadian hydropower components under seismic loading", *9th Canadian Conference on Earthquake Engineering*, Ottawa, Ontario, Canada.

Londe, P. and Lino, M. (1992), "Hard fill dam, the faced symmetrical Hard fill dam a new concept for RCC", *Int. Water Pow. Dam Constr.*, **44**, 19-24.

McCann, Jr., Franzini, J.B. and Shah, H.C. (1983a), "Preliminary safety evaluation of existing dams", Department of Civil Engineering, Stanford University.

McCann, Jr., Franzini, J.B. and Shah, H.C. (1983b), "Preliminary safety evaluation of existing dams", Department of Civil Engineering, Stanford University.
Mirzahossein Kashani, S. and Ghaemian, M. (2009), "Seismic fragility assessment of concrete gravity dams", *29th Annual USSD Conference*, Nashville, Tennessee.
Mita, A. and Takahira, S. (2004), "Damage index sensor for smart structures", *Struct. Eng. Mech.*, **17**(3-4), 331-346.
Nateghi, F. and Shahsavar, V. (2004), "Development of fragility and reliability curves for seismic evaluation of a major pre stressed concrete bridge", *13th World Conference on Earthquake Engineering*, Vancouver, Canada.
Raphael, J.M. (1970), "The optimum gravity dam. Rapid construction of concrete dams", ASCE, New York, 221-247.
Roy, J., Tremblay, R. and Leger, P. (2015), "Torsional effects in symmetrical steel buckling restrained braced frames: Evaluation of Seismic design provisions", *Earthq. Struct.*, **8**(2), 423-442.
Shahriar, A., Modirzadeh, M., Sadiq, R. and Tesfamariam, S. (2012), "Seismic induced damageability Evaluation of steel buildings: a Fuzzy-TOPSIS method", *Earthq. Struct.*, **3**(5), 695-717.
Tekie, P.B. and Ellingwood, B.R. (2003), "Seismic fragility assessment of concrete gravity Dams", *Earthq. Eng. Struct. Dyn.*, **32**(14), 2221-2240.
Yang, S.H. and Yishan, L. (1981), "Water control", Beijing, Xinhua Publishing House, 562-575.

*CC*